Preprint
UCRL-JC-135607

Micromagnetic Simulations of Submicron Cobalt Dots

G.J. Parker, C. Cerjan

This article was submitted to the 44th Annual Conference on Magnetism and Magnetic Materials, San Jose, CA, November 15-18, 1999

August 30, 1999

U.S. Department of Energy

Lawrence Livermore National Laboratory

MICROMAGNETIC SIMULATIONS OF SUBMICRON COBALT DOTS

G.J. Parker and C. Cerjan

Lawrence Livermore National Laboratory, 7000 East Avenue, L-395, Livermore, CA 94550.

Abstract

Numerical simulations of submicron Co extruded elliptical dots were performed to illustrate the relative importance of different physical parameters on the switching behavior in the easy direction. Shape, size, magnetic moment magnitude and crystalline anistropy, both magnitude and distribution, were varied. The simulation includes calculation of the magnetostatic, exchange and crystalline anistropy fields on a structured mesh using finite difference techniques. The smooth boundary of the dots are accurately represented by use of the Embedded Curve Boundary method.

PACS: 75.40Mg, 75.50.-d, 85.70.-w

Keywords: Micromagnetic simulation, Co dots, magnetic reversal, magnetic vortex.

Corresponding Author:

Charles Cerjan

Lawrence Livermore National Laboratory

7000 East Avenue, L-395

Livermore, CA 94551

(925) 423-8032, (925) 423-1488 (FAX)

cerjan1@llnl.gov

I. Introduction

Mircomagnetics is an approximation [1] useful for modeling the behavior of small scale (anti-)ferromagnetic materials. This continuum approximation efficiently and accurately models the response of magnetic materials for important commercial and industrial applications, including but not limited to read/write heads for magnetic storage, properties and performance of magnetic storage media, and non-volatile magnetic random access memory (MRAM). Furthermore, such simulations not only offer detailed information on the interactions of various physical mechanisms affecting their response, but also holds the potential of increasing the fundamental understanding of micromagnetic materials.

In this paper, we perform a series of simulations using a previously reported algorithm [2]. Briefly, this algorithm uses a structured (orthogonal Cartesian 3-D) mesh to calculate the magnetostatic and exchange fields by finite differences. Smooth curved boundaries are included in the algorithm by approximating the curved boundary by sub-mesh piecewise linear line segments which, when combined with the basic boundary conditions of the magnetic field, give rise to modified finite differencing equations as described in Ref. 2. Once the appropriate fields are calculated, the Landau-Liftshitz-Gilbert equation is semi-implicitly advanced in time. The two calculations (field and magnetic moment relaxation) are repeated until user specified criteria are reached. The algorithm was shown to be fast and robust and agree well with other simulations' results. [2]

Here we are concerned about the magnetic response of submicron polycrystalline Cobalt elliptical dots of varying thickness ($16-40$ nm) along the easy direction. The dots have major and minor axes of $a = 450$ nm and $b = 250$ nm, respectively. The magnetic moment, M_s, derived from experiment ranged from 1160 to 1450 emu/cm^3. An exchange coupling coefficient of $A = 1.6 \times 10^{-6}$ erg/cm^2 along with the crystalline anistropy coefficient of $K = 7.5 \times 10^5$ erg/cm^3 and a nominal grain size of 6 nm were also taken from experimental results. Detailed experimental procedures and results can be found in [3].

As shown previously, good agreement between simulation and experiments were obtained independent of the 2-D or 3-D [2,4] random distribution of the crystalline anistropy, $\hat{k}$, for the magnetic

response in the easy direction. Experimentally, the switching of the dots were seen to originate from a nucleation of a single or double vortex in the magnetic configuration at small values of an uniformly applied external field. Larger fields were then needed to completely switch the magnetic configuration. Simulation results predicted both the coercivity and the required external field needed to completely switch the magnetic configuration. However, the simulation predicted that single vortex formation occurs 50% of the time instead of the much larger experimentally observed 97%. Furthermore, unlike the experimental result of a gradual nucleation of the single vortex state at low applied fields, simulations predict a sudden onset of the vortex state near the coercivity field, H_c.

In order to illustrate the effects of different physical parameters on the magnetic response, we have varied numerous parameters in the simulations to determine the relative importance of each. The physical parameters varied include: shape and size of the dots, the magnetic moment M_s, the magnitude of the crystalline anistropy K, the direction of the crystalline anistropy $\hat{k}$ and the grain size and coupling. The exchange field coefficient A was not varied and was fixed to 1.6×10^6 erg/cm^2.

In all the simulations reported here, the ellipse was centered on the uniformly discretized mesh. The easy direction (i.e. the major axis) was placed along the x-axis while the minor axis was along y. The mesh spacing in the z direction was adjusted so that 10 computational cells resided in the thickness of the dot. The x and y mesh spacing was fixed at 6 nm. Around this uniformly discretized mesh, geometrically increasing mesh size of 20 cells in each of the 6 directions were placed so that the total length was much larger than any of the dot length scales. This was required to have a Dirichlet boundary condition of zero at 'infinity' for the magnetostatic potential calculation. An external uniform applied field along the x-axis was used to invoke the magnetic response of the dots. All dots were initially given a magnetic moment configuration of a single vortex.

The organization of this presentation is straightforward. In Section II, the effects of shape/size of the dots and the magnitude of the magnetic moment on the magnetic response is first performed. Section III shows the effect of uniform distributions of the crystalline anistropy on the magnetic

response. Finally, Section IV shows some effects of different random orientations of the crystalline anistropy.

II. Shape, Size and Magnetic Moment Magnitude

In this section, a series of simulations on 30 nm tall dots were performed with out any crystalline anistropy, $K = 0$. All of these simulations produced a hysteresis loop (that is $\langle M_x \rangle$ as a function of applied field) that were 'square'- the magnetic moment configuration switched abruptly at H_c.

Table I is the summary of results for this series of simulations. The base case (Run 1) uses the experimentally determined size and the bulk value of M_s for Co. Experimental results suggest that the effective M_s may be as much as 80% lower in the dots and Run 2 uses this smaller value. We see that varying M_s has little or essentially no affect on H_c to within the resolution of the stepping of the applied field in these runs (20 Oe).

Runs 3 and 4 reduce size of the dots by 10% in each direction, but keeps the eccentricity (a/b) the same. As expected, H_c increases by 8% compared to the standard size. This is reasonable since the smaller dots have a larger demagnetization field and therefore take a larger external field to invoke the switching behavior. This is also confirmed by the fact that the magnetostatic energy for the smaller dots increased $\sim$20%.

Finally, Runs 5 and 6 change the shape of the dots by reducing the eccentricity by 10% but keeps the volume of the dot the same. This small change of shape leads to the largest change of H_c for this series of simulations with $K = 0$. The reduction of $\sim$ 25% is not unexpected since more circular cross section allows for domain walls to form and propagate easier.

III. Uniform Distributions of Crystalline Anistropy

In this section, another series of simulations on 30 nm tall dots were performed. We fix the magnitude of the crystalline anistropy K to 7.5×10^5 erg/cm^3 but vary the orientation to be uniform along one of the Cartesian axis.

Table II is the summary of results for this series of simulation. For $\hat{k}$ along the x axis (Runs 7-12), we see that H_c increases compared to when $K = 0$. This unsurprising result is due to the crystalline anistropy 'freezing' the magnetic moments along the applied field direction, requiring an larger applied field to reverse the magnetic configuration. More interesting, reducing M_s increases H_c. This is understandable since the maximum crystalline anisotropic field

$$\mathbf{H}_k = \frac{2K}{M_s^2}\left(\mathbf{M}\cdot\hat{k}\right)\hat{k} \tag{1}$$

increases with decreasing M_s. Smaller dot size (Runs 9 and 10) or changing the shape (Runs 11 and 12) scaled almost precisely as when $K = 0$. Though, since the values of H_c increased, changing the shape only decreased H_c by 15% compared to the standard size.

When $\hat{k}$ is along the z-axis, it has minimal affect on H_c. It may decrease H_c slightly for the larger M_s runs. This weak response is not unexpected since the demaginzation field in the z direction is very large due to the small thickness of the dots. Once the magnetic moments try to rotate out of the xy plane, a very large opposing field is created in these thin structures.

However, when $\hat{k}$ is along the y-axis, more complicated behavior is seen. First, H_c drops remarkably for all cases and, unlike the previous trends, the lower M_s decreases H_c. Again, this is reasonable since now $\mathbf{H}_k$ is larger and reinforces the turning of the magnetic moments away from the applied field. Unlike the previous case, there is no resulting opposing field to stop the rotation. The exchange couple fields then forces the entire magnetic moment configuration to form a singe vortex. Changing the shape of the dot not only produces a $H_c = 0$, but the onset of the single vortex actually occurs before the applied field switches signs (the numbers in '()' in Table II).

When $\hat{k}$ lies along the x or z-axis, the resulting hysteresis loops are square as when $K = 0$. However, when along the $y - axis$, H_c is very small and all simulations report a formation of a single vortex in the magnetic configuration. This single vortex persists until a large enough external field ($\sim$ 1300 Oe) when it's finally annihilated. Figure 1 shows a typical case.

IV. Random Distributions of Crystalline Anistropy

In this section, we allow the crystalline anistropy distribution $\hat{k}$ to have random distributions. Unlike the previous results where the simulations were reproducible, multiple simulations with random $\hat{k}$ have to be done since results can vary dramatically from one random distribution to another. This fact is, perhaps, one of the most important conclusions of this section. Given the identical problem, including the probability function for generating the random $\hat{k}$ distributions, different distributions not only affect H_c but also lead to either single or double vortex formation. (Of course, given the identical $\hat{k}$ distribution, the simulation returns the same results. That is, the algorithm itself is deterministic.)

Table III shows some results of different $\hat{k}$ distribution functions for the 30 nm thick dot. Identical entries mean only a different distribution was realized. All runs have $K = 7.5 \times 10^5$ erg/cm^3.

'3-D' (Runs 25 and 26) means that $\hat{k}$ is isotropically random in 3-D for each grain. As shown previously [2], higher M_s values produce double vortex configuration and too low H_c while lower M_s tend to produce accurate H_c predictions and about half single vortex patterns. '2-D' (Runs 27 and 28) means that $\hat{k}$ is random in the xy plane and identically zero in z. Not surprisingly, the results do not change appreciably, except that H_c increases slight. This is due to the fact that in 2-D it is more likely that any particular grain will have $\hat{k}$ along x compared to a 3-D distribution. We have seen that $\hat{k}$ along x increases H_c. Halving the grain size (Run 29) didn't affect the H_c, but did tend to produce more single vortex configuration at switching. Figure 1 shows the averaged magnetic response for those simulations that produced single vortex states for both 2-D and 3-D configurations.

Reducing the size of the dots (Runs 30 and 31) resulted in higher H_c for the lower M_s values. Higher M_s values still produced small H_c compared to experiment. Changing the shape (Run 32) seem to suggest that even for the lower M_s value, H_c is underestimated by large factors.

The final run (33) tried to duplicate TEM pictures of the grain structure of the dots [10]. From those scans, the grains appear to grow mostly along the z-axis offset by a small random angle. It was also seen that in the vast majority of the grains grew in pairs and it was suggested [10] that the

$\hat{k}$ were coupled, or 'twinned', in these grains to be in opposite directions. Run 33 was produced by generating a random distribution of $\hat{k}$ in the xy plane and a probability distribution for the polar angle, $\theta = \cos^{-1}\mu$ given by:

$$\frac{2\left(\mu - \mu_l\right)}{\left(1 - \mu_l\right)^2} \tag{2}$$

where $\mu_l = 3\langle\mu\rangle - 2$ and $\langle\mu\rangle$ is the average cosine of the polar angle in this distribution ($\theta = 20^o$ here). Integrating the above equation from μ_l to μ and setting the result to a uniformly distributed random number $[0 - 1]$ and solving for μ gives the required random k_z. Not only do the results agree well with experiment for H_c, but all runs produced a single vortex. A typical result (labeled "twinned") is shown in Figure 1.

Increasing the value of K to the bulk value of Co were also performed. Unfortunately in most cases the results in H_c did not come close to experimental results, typically much too large. Of those which did, typically very complex vortex behavior was seen. However, most of these runs did exhibit early and slow nucleation of the switching configuration.

V. Conclusion

In this paper, we have done numerical studies on polycrystalline Cobalt elliptical dots and their switching behavior. By simplify the real dots by first ignoring the crystalline anistropy and then using simple (uniform) distributions, insight has been gained on how the shape, size and magnetic moment magnitude affects the switching field and magnetic configuration.

Random distributions of the crystalline anistropy were then implemented. Different distributions (generated from the same probability function) generated different magnetic responses of the dots. Slow nucleation of the magnetic configuration were only realized with large values of the crystalline anistropy coefficient which rarely lead to the observed coercivity and magnetic configuration.

Acknowledgments

This work was performed under the auspices of the United States Department of Energy by Lawrence Livermore National Laboratory under Contract W-7405-ENG-48.

References

1. W.F. Brown, "Micromagnetics", John Wiley & Sons, New York, 1963.

2. G.J. Parker, C. Cerjan and D.W. Hewett, "Embedded curve boundary method for micromagnetic simulations", submitted to *J. Magn. Magn. Mater.*

3. A. Fernandez, M.R. Gibbons, M.A. Wall and C.J. Cerjan, *J. Magn. Magn. Mater.*, **190**, 71, (1998); A. Fernandez. and C.J. Cerjan, *Appl. Phys. Lett. (to appear).*

4. M.R. Gibbons, G.J. Parker, C.J. Cerjan and D.W. Hewett, "Finite difference micromagnetic simulation with self-consistent currents and smooth surfaces", *J. Appl. Phys. (to appear).*

Table I: Shape, size and M_s effects

Run	M_s (emu/cm^3)	a (nm)	b (nm)	H_c (Oe)
experiment	1160 - 1450	450	250	200
1	1450	450	250	1250
2	1160	450	250	1230
3	1450	405	225	1350
4	1160	405	225	1330
5	1450	436.4	272.7	930
6	1450	436.4	272.7	950

Table II: Uniform crystalline anistropy effects

Run	$\hat{k}$	M_s (emu/cm^3)	a (nm)	b (nm)	H_c (Oe)
7	$\hat{x}$	1450	450	250	2210
8	$\hat{x}$	1160	450	250	2430
9	$\hat{x}$	1450	405	225	2330
10	$\hat{x}$	1160	405	225	2530
11	$\hat{x}$	1450	436.4	272.7	1910
12	$\hat{x}$	1160	436.4	272.7	2150
13	$\hat{z}$	1450	450	250	1150
14	$\hat{z}$	1160	450	250	1210
15	$\hat{z}$	1450	405	225	1230
16	$\hat{z}$	1160	405	225	1310
17	$\hat{z}$	1450	436.4	272.7	910
18	$\hat{z}$	1160	436.4	272.7	950
19	$\hat{y}$	1450	450	250	150
20	$\hat{y}$	1160	450	250	10
21	$\hat{y}$	1450	405	225	230
22	$\hat{y}$	1160	405	225	0 (50)
23	$\hat{y}$	1450	436.4	272.7	0 (370)
24	$\hat{y}$	1160	436.4	272.7	0 (370)

Table III: Random distrubtions of crystalline anistropy effects

Run	$\hat{k}$	M_s (emu/cm^3)	a (nm)	b (nm)	H_c (Oe)	Double or Single vortex
Expt.			~ 450	$\sim$250	200	S
25	3-D	1450	450	250	20	D
	3-D	1450	450	250	40	D
26	3-D	1160	450	250	254	D
	3-D	1160	450	250	196	S
	3-D	1160	450	250	215	S
	3-D	1160	450	250	195	D
	3-D	1160	450	250	254	D
27	2-D	1450	450	250	26	S
	2-D	1450	450	250	58	D
28	2-D	1160	450	250	236	S
	2-D	1160	450	250	234	D
	2-D	1160	450	250	235	D
	2-D	1160	450	250	234	S
29	3-D, half grain	1160	450	250	176	D
	3-D, half grain	1160	450	250	216	S
	3-D, half grain	1160	450	250	197	S
	3-D, half grain	1160	450	250	196	S
	3-D, half grain	1160	450	250	176	D
30	3-D	1450	405	225	76	D
	3-D	1450	405	225	17	S
31	3-D	1160	405	225	256	D
	3-D	1160	405	225	293	S
32	3-D	1160	436.4	272.7	58	D
	3-D	1160	436.4	272.7	37	S
33	twinned	1160	450	250	178	S
	twinned	1160	450	250	187	S

Figure Captions

Fig. 1. Magnetic response of 30 nm thick Co dot: $a = 450$ nm, $b = 250$ nm, $M_s = 1160$ emu/cm^3 and $K = 7.5 \times 10^5$ erg/cm^3. See text for details.

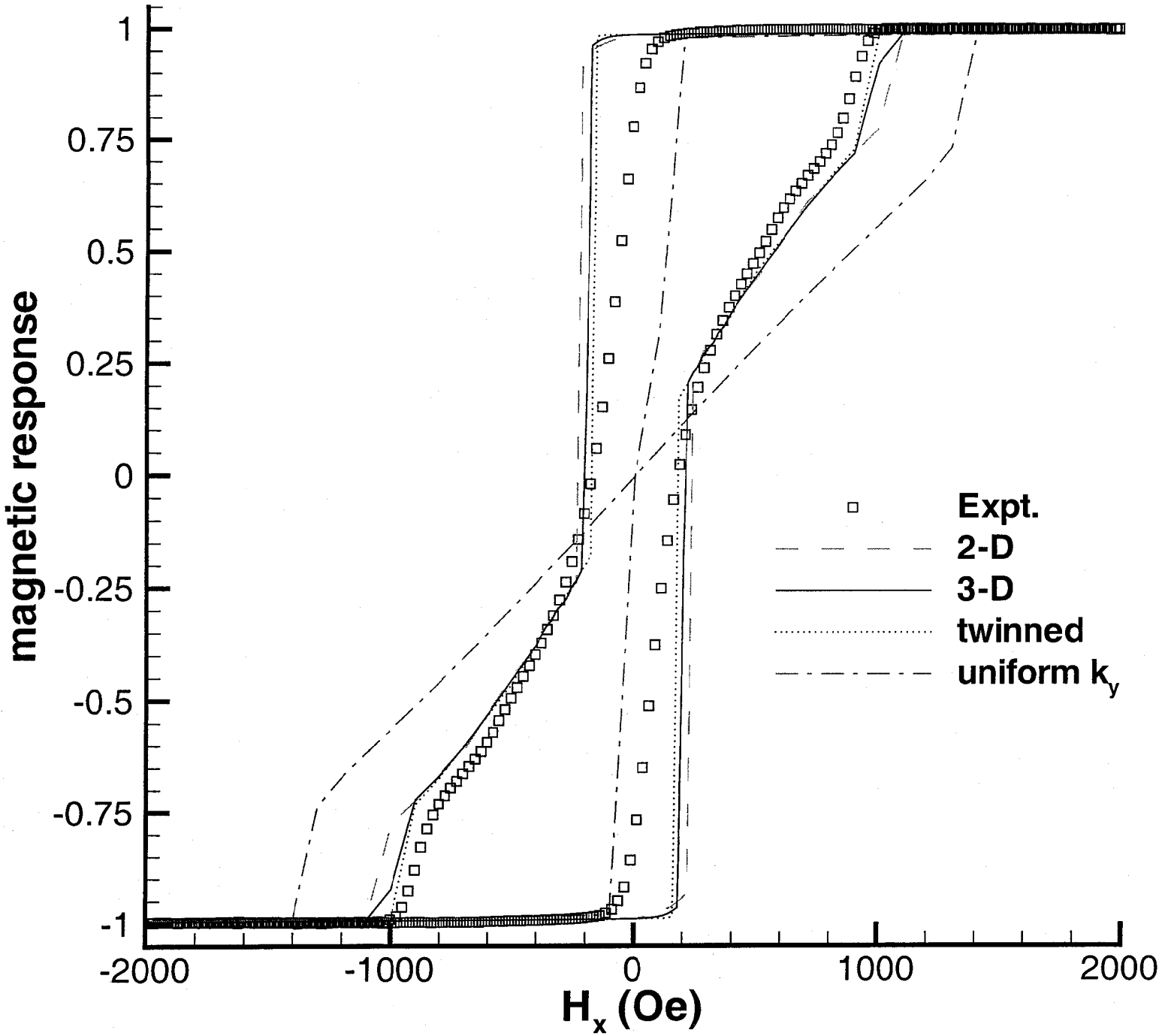
magnetic response
1
0.75
0.5
0.25
0
-0.25
-0.5
-0.75
-1
-2000
-1000
0
1000
2000
H_x (Oe)
Expt.
2-D
3-D
twinned
uniform k_y